ON THE USE OF ORTHOTROPIC YIELD SURFACES TO OBTAIN LIMIT LOADS FOR PERFORATED PLATES

A. SAWCZUK

Department of Continuous Media, Institute of Fundamental Problems of Technology, Polish Academy of Sciences, Warsaw, Poland

W.J. O'DONNELL

Engineering Design and Analysis Services, O'Donnell & Associates, Inc., Pittsburgh, Pennsylvania 15232, U.S.A.

and

J. POROWSKI

Prosynchem, Gliwice, Poland

Visiting Research Fellow, O'Donnell & Associates, Inc., Pittsburgh, Pennsylvania 15232, U.S.A.

SUMMARY

Uniformly loaded circular plates having orthotropic plastic properties are investigated. Limit pressure solutions are obtained for both the simply supported and rigidly built-in edge conditions. The usual sandwich plate theory is used. Statically admissible radial and circumferential bending moment fields are found for all annular regions of the plates, and the associated velocity fields are shown to be kinematically admissible. Numerical results are given in dimensionless form covering arbitrary plate geometries over the entire range of material orthotropy.

These solutions are quite useful in the plastic design and analysis of perforated plates used as pressure vessel heads, tube sheets, reactor core support plates and the like. Perforated plates have considerably higher effective yield strengths when subjected to equi-biaxial loading than when subjected to loading of arbitrary biaxiality and orientation with respect to the penetration pattern. Thus, the equivalent orthotropic plastic material concept is ideally suited to the analysis of such plates. The resulting limit load pressures are substantially lower than the values obtained using isotropic Tresca yield properties based on the yield strength for equi-biaxial loading. The results are substantially higher than the values obtained using the maximum isotropic Tresca yield properties falling entirely within the orthotropic yield surface.

This work was sponsored by the Pressure Vessel Research Committee of the Welding Research Council.

Nomenclature

A = outer radius of the plate

C_i = integration constants

$2k$ = yield stress of solid isotropic material in uniaxial tension

M_r, M_θ = radial and tangential moments per unit length

M_o = reference moment , $M_o = k\mu\varsigma_o T^2/2$

m_r, m_θ = dimensionless radial and tangential moments

P = pressure

p = dimensionless pressure defined by equation /10/

R = radial coordinate

r = dimensionless coordinate r=R/A

r_B = dimensionless radius of interface between the plastic regions yielding in regimes AB and BC of Fig. 1

r_C = dimensionless radius of interface between the plastic regions yielding in regimes BC and CD of Fig. 1

T = plate thickness

$\dot{w}$ = deflection velocity

w_o = constant used to define velocity fields

Y_{ii} = the yield stresses of equivalent orthotropic material in uniaxial tension in directions of orthotropy, i = 1,2,3, no sum

Y = yield point of the equivalent solid material for uniaxial in-plane loading

β = orthotropy coefficient defined by equation /1/

$\varsigma_r, \varsigma_\theta$ = dimensionless radial and tangential stresses for plane stress conditions

ς_o = general cut-out factor

μ = ligament efficiency , $\mu = h/P_t$

h = width of minimum ligament section

σ_{ii} = principal stresses in directions of orthotropy, i=1,2,3,no sum

$\varkappa_r, \varkappa_\theta$ = dimensionless curvatures

ϕ = yield function given by equation /7/

χ = auxiliary parameter used in equations /18/ and /19/

ν = positive scalar in flow law equations /8/

$\cdot$ = denotes time rates

1. Introduction

The solution of an elastic-plastic problem of perforated circular plate in bending obtained in Ref. [1] was based on the concept of an equivalent isotropic material. Since the sandwich construction of the plate was considered, the plastic behavior of the perforated sheet subjected to biaxial in-plane loading and plane stress conditions was analyzed. The equivalent isotropic material was described by the Tresca hexagon inscribed within the lower bound yield surfaces for perforated sheets subjected to biaxial in-plane loading of arbitrary orientation with respect to the penetration pattern.

The concept of an equivalent orthotropic material is presented herein.

This concept is applied in the limit analysis of circular perforated plates. The so-called "general cut-out" factor, derived in Refs. [2] and [3] for the perforated materials with equilateral triangular penetration patterns, is used to describe the plastic properties of the equivalent orthotropic plastic material. Uniformly loaded circular plates of equivalent orthotropic plastic materials are then investigated. The solutions are obtained for rigid-plastic material behaviour for the cases of simply supported and built-in edge conditions. It is shown that the collapse loads obtained using the concept of an equivalent orthotropic material are significantly higher than those obtained for isotropic plates.

2. Yield Surfaces for Equivalent Orthotropic Material

A piecewise linear theory of plasticity of anisotropic materials was formulated in Ref. [4]. The yield surface for incompressible materials is represented in the space of principal stresses by parallelepipedes whose edges are parallel to the axis of hydrostatic pressure. The equivalent orthotropic material considered herein is described in Fig. 1. The stress in the transverse direction is zero and the yield properties are independent of the direction of loading in the plane. $Y_{11} = Y_{22}$ are then determined by uniaxial in-plane loading. Y_{33} is the yield stress for equi-biaxial in-plane loading.

The plastic properties of the equivalent solid material may then be conveniently described by the two constants Y and β where:

$$Y = Y_{11} = Y_{22} \quad \text{and} \quad Y = \beta Y_{33} \qquad /1/$$

The extent to which β differs from unity indicates the degree of orthotropy. The dashed line of Fig. 1 shows the yield surface of an isotropic material for which $Y_{11} = Y_{22} = Y_{33} = Y$. The orthotropic equivalent solid material described in Fig. 1 is precisely analogous to a solid material having isotropic in-plane yield properties, but higher yield properties for loading in the transverse direction. The plane stress generalized Tresca yield condition for this equivalent transversally isotropic material is defined by the equations:

$$|\sigma_{11} - \sigma_{22}| = Y \qquad \text{for regime FE and BC} \qquad /2a/$$

$$|(\beta-1)\sigma_{11} + \sigma_{22}| = Y \qquad \text{for regime AB and DE} \qquad /2b/$$

$$|\sigma_{11} + (\beta-1)\sigma_{22}| = Y \qquad \text{for regime AF and CD} \qquad /2c/$$

where σ_{11}, σ_{22} are the in-plane stresses in the unperforated material. For perforated materials, the yield point for equi-biaxial in-plane stress is always larger than the yield point for uniaxial loading, $\beta < 1$. Hence the requirement that the yield surface must be convex will always be satisfied.

3. Generalized Stresses

Since the lower bound approach is used to derive the plastic properties of the equivalent orthotropic material, its yield surface must fall entirely within the yield surface of the perforated material. The yield point in uniaxial tension Y and the yield point for the equi-biaxial state of stress $Y_{33} = Y/\beta$ must be obtained for the perforated materials. For equilateral penetration patterns /i.e. triangular or square/ and equi-biaxial loading, the minimum ligament sections can support the yield strength of the solid material. This is shown in Ref.[2] for the equilateral triangular pattern and can easily be seen for the square penetration pattern. Consequently,

$$Y_{33} = 2\mu k \qquad /3/$$

where μ is the ligament efficiency.

The minimum yield strength for a perforated sheet subjected to uniaxial stress arbitrarily oriented with respect to the penetration pattern may be defined by the so-called cut-out factor ϱ_o described in Refs.[2] and [3]. The minimum yield point for uniaxial loading of the equivalent solid material is given by:

$$Y = 2\mu k \varrho_o \qquad /4/$$

For a triangular penetration pattern a lower bound to the equivalent yield stress is plotted in Fig. 2 versus the ligament efficiency.

Relation /4/ defines the maximum size of the Tresca hexagon which may be inscribed within the yield surface of the orthotropic material and used as reference for dimensionless stresses. It is apparent that for the penetration patterns which were considered, $\varrho_o = \beta$ which means that general cut-out factor ϱ_o represents directly the degree of orthotropy. The yield condition for the equivalent transversally isotropic material in plane stress is given by:

$$\max\left\{|\varrho_r - \varrho_\theta|,\ |(\varrho_o-1)\varrho_r + \varrho_\theta|,\ |\varrho_r + (\varrho_o-1)\varrho_\theta|\right\} = 1 \qquad /5/$$

where ϱ_r and ϱ_θ are the dimensionless stresses σ_{11}/Y and σ_{22}/Y, respectively. The graphical representation of the limit surfaces employed with this concept are shown in Fig. 3.

For the perforated plate in bending, the bending moments can be defined as stress resultants

$$m_r = M_r/M_o \ , \quad m_\theta = M_\theta/M_o \qquad /6/$$

where M_o is a reference yield moment associated with the yield stress /4/.

The yield condition in the space of generalized stresses is given by:

$$\phi = \max\left\{|m_r - m_\theta|,\ |m_\theta + (\varrho_o-1)m_r|,\ |m_r + (\varrho_o-1)m_\theta|\right\} = 1 \qquad /7/$$

Curvatures as generalized strains can be obtained for each side of the yield polygon from the plastic potential flow law. Dimensionless moment-curvature rate relations are

$$\dot{\kappa}_r = -\frac{d^2\dot{w}}{dr^2} = \nu\frac{\partial\phi}{\partial m_r} \quad , \quad \dot{\kappa}_\theta = -\frac{1}{r}\frac{d\dot{w}}{dr} = \nu\frac{\partial\phi}{\partial m_\theta} \qquad /8/$$

where ν is an arbitrary positive scalar.

4. Simply Supported Circular Plate

The solution for uniformly loaded plates whose orthotropy is characterized by three yield points is given in general form in Ref. 5 . For the considered material /$Y_{11} = Y_{22} = Y$ and $\frac{Y}{Y_{33}} = \beta = \varrho_o$/ the entire plate during collapse remains in the regime $m_\theta + (1-\varrho_o)m_r = 1$. The collapse pressure for the simply supported edge condition is given by the relation:

$$p = \frac{1}{3} + \frac{2}{3\varrho_o} \qquad /9/$$

where p is the dimensionless pressure:

$$p = \frac{PA^2}{6M_o} \qquad /10/$$

The moment distribution is given by

$$m_r = \frac{1}{\varrho_o}(1-r^2) \quad , \quad m_\theta = \frac{1}{\varrho_o} + \left(1-\frac{1}{\varrho_o}\right)r^2 \qquad /11/$$

and kinematically admissible velocity field has the form

$$w = w_o\left(1-r^{\varrho_o}\right) \qquad /12/$$

5. Built-in Plate

The built-in plate will yield in three of the stress regimes specified in equation /7/. The respective regimes will be labelled AB, BC and CD with reference to the yield polygon in Fig. 1. The equilibrium equations are as follows:

$$\frac{d}{dr}(rm_r) + (\varrho_o - 1)m_r - 1 = -3pr^2 \qquad \text{for regime AB} \qquad /13a/$$

$$\frac{d}{dr}(rm_r) + m_r - 1 = -3pr^2 \qquad \text{for regime BC} \qquad /13b/$$

$$\frac{d}{dr}(rm_r) + \frac{1}{1-\varrho_o}(m_r - 1) = -3pr^2 \qquad \text{for regime CD} \qquad /13c/$$

after integration respectively:

in regime AB: $$m_r = \frac{1}{\varrho_o} - \left(\frac{3p}{2+\varrho_o}\right)r^2 \qquad /14a/$$

in regime BC: $$m_r = \ln r - \left(\frac{3\mu}{2}\right) r^2 + C_2 \qquad /14b/$$

in regime CD: $$m_r = -\frac{1}{\varrho_o} - \left(\frac{3\mu(\varrho_o-1)}{3\varrho_o-2}\right) r^2 + C_3 r^{\left(\frac{\varrho_o}{\varrho_o-1}\right)} \qquad /14c/$$

The condition resulting from symmetry for regime A,

$$m_r(0) = m_\theta(0) = \frac{1}{\varrho_o} \qquad /15/$$

whereas the boundary and interface conditions for regimes B, C, D are:

$$m_r(1) = m_\theta(1) = -\frac{1}{\varrho_o} \; ; \quad m_r(r_B) = 0 ; \quad m_r(r_C) = -1 \qquad /16/$$

The continuity requirements on the interfaces are:

$$m_r(r_B)\big] = 0 \; , \quad m_r(r_C)\big] = 0 \qquad /17/$$

where r_B and r_C denote dimensionless radii determining the interfaces between the stress regimes, and the symbol] indicates the discontinuity across the interfaces. The dimensionless radii r_B and r_C, and the collapse pressure p, can now be obtained in terms of the general cut-out factor using relations /15/ thru /17/ in equations /14/:

$$\ln\left[\frac{(3\varrho_o-2)\chi}{\varrho_o+2}\right] = \frac{(3\varrho_o-2)\chi}{\varrho_o} - 3 - \frac{2}{\varrho_o} \qquad /18/$$

$$\mu = \left[\frac{3\varrho_o-2}{3\varrho_o r_C^2}\right]\chi \qquad /19/$$

$$r_B = \left[\frac{1}{3\mu}\left(1+\frac{2}{\varrho_o}\right)\right]^{1/2} \qquad /20/$$

where $$\chi = \frac{1}{1 - r_C^{\left(\frac{3\mu-2}{1-\varrho_o}\right)}}$$

The bending moment field takes eventually the form

for regime AB $$m_r = \frac{1}{\varrho_o} - \left(\frac{3\mu}{\varrho_o+2}\right) r^2 \; , \quad m_\theta = \frac{1}{\varrho_o} + \left[\frac{(\varrho_o-1)3\mu}{\varrho_o+2}\right] r^2 \; , \qquad /21/$$

for regime BC $$m_r = \ln\left(\frac{r}{r_B}\right) - \frac{3\mu}{2}\left(r^2 - r_B^2\right) \; , \quad m_\theta = m_r + 1 \; , \qquad /22/$$

for regime CD $$m_r = -\frac{1}{\varrho_o} + \left[\frac{3\mu(\varrho_o-1)}{3\varrho_o-2}\right] \cdot r^2 \cdot \left[1 - r^{\left(\frac{2-\varrho_o}{\varrho_o-1}\right)}\right] , \qquad /23/$$

$$m_\theta = -\frac{1}{\varrho_o} + \left(\frac{3\mu}{3\varrho_o-2}\right) \cdot r^2 \cdot \left[1 - r^{\left(\frac{2-\varrho_o}{\varrho_o-1}\right)}\right] .$$

The plotted values of parameters r_B and r_C are shown in Fig. 4 versus the general cut-out factor which describes the degree of orthotropy of the plate. For $\varrho_o \to 1$, which represents the isotropic behavior of the material, r_C tends to unity which shows that the plastic region in regime CD vanishes, and the radius r_B tends to 0.730 which is the value obtained for built-in isotropic plates.

To demonstrate that the solution obtained by considering the equilibrium conditions is also kinematically admissible, the associated velocity fields must be derived. Eliminating parameter ν from relations /8/ for each side of the yield polygon, integrating and using the boundary and continuity conditions the resulting velocity fields during plastic flow become in regime AB:

$$\dot{w} = w_o r_C^{\left(\frac{\varrho_o}{\varrho_o-1}\right)} \frac{1}{\varrho-1}\left[\left(\frac{r}{r_B}\right)^{\varrho_o} - \varrho_o \ln\left(\frac{r_C}{r_B}\right) - (\varrho_o-1) r_C^{\left(\frac{\varrho_o}{1-\varrho_o}\right)} + \varrho_o - 2\right] \qquad /24a/$$

in regime BC: $$\dot{w} = w_o r_C^{\left(\frac{\varrho_o}{\varrho_o-1}\right)}\left[1 - \frac{\varrho_o}{\varrho_o-1} \ln\left(\frac{r_C}{r}\right) - r_C^{\left(\frac{\varrho_o}{1-\varrho_o}\right)}\right] \qquad /24b/$$

in regime CD $$\dot{w} = w_o \left[r^{\left(\frac{\varrho_o}{\varrho_o-1}\right)} - 1\right] \qquad /24c/$$

where w_o is a parameter. This mechanism of collapse is kinematically admissible and corresponds to the previous assumption that the plate yields in stress regime ABCD. Hence, the exact solution of the considered limit analysis problem has been obtained.

The collapse pressure, and moment distribution are shown in Figs. 5 and 6, respectively. The plots are made versus the general cut-out factor ϱ_o. Its numerical values for the plates with equilateral triangular penetration patterns are given in Ref. [2]. Much smaller cut-out factors would be expected for square penetration patterns.

In Fig. 7 comparison of collapse pressure for isotropic and orthotropic plates is shown for triangular penetration pattern.

References

[1] POROWSKI, J., O'DONNELL, W.J., "Elastic-Plastic Bending of a Constrained Circular Perforated Plate under Uniform Pressure /Triangular Penetration Pattern/" to be published in the Welding Research Council Bulletin.

[2] O'DONNELL, W.J. and POROWSKI, J., "Yield Surfaces for Perforated Materials", presented at the Applied Mechanics Conference in La Jolla, California, June, 1972, ASME Paper No. 72-APM-41, to be published in the Journal of Applied Mechanics.

[3] POROWSKI, J. and O'DONNELL, W.J., "Effective Plastic Constants for Perforated Materials", approved by the Pressure Vessel Research Committee for publication.

[4] SAWCZUK, A., "Linear Theory of Plasticity of Anisotropic Bodies and Its Applications to Problems of Limit Analysis", Arch. Mech. Stos., 5, 11 /1959/ 541-557.

[5] SAWCZUK, A., JAEGER, T., "Grenztragfähigkeits-Theorie der Platten", Springer-Verlag, Berlin, 1963.

[6] SAWCZUK, A., "Some Problems of Load Carrying Capacities of Orthotropic and Non-Homogeneous Plates", Arch. Mech. Stos., 4, 8 /1956/, 549-563.

[7] SAWCZUK, A., "On the Theory of Anisotropic Plates and Shells", Arch. Mech. Stos., 3, 13 /1961/ 355-365.

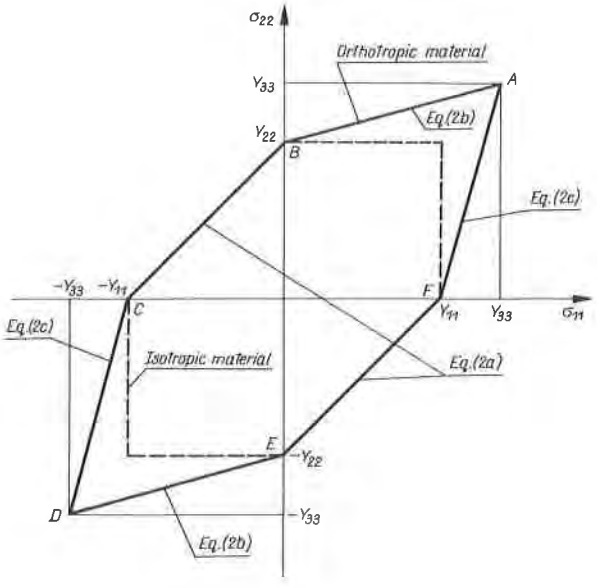

FIGURE 1 YIELD SURFACE FOR ORTHOTROPIC MATERIAL

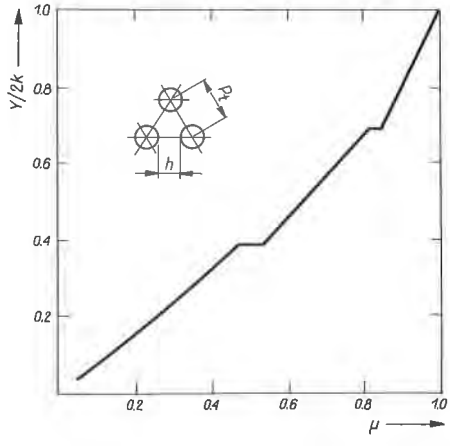

FIGURE 2 YIELD STRESS FOR EQUIVALENT MATERIAL

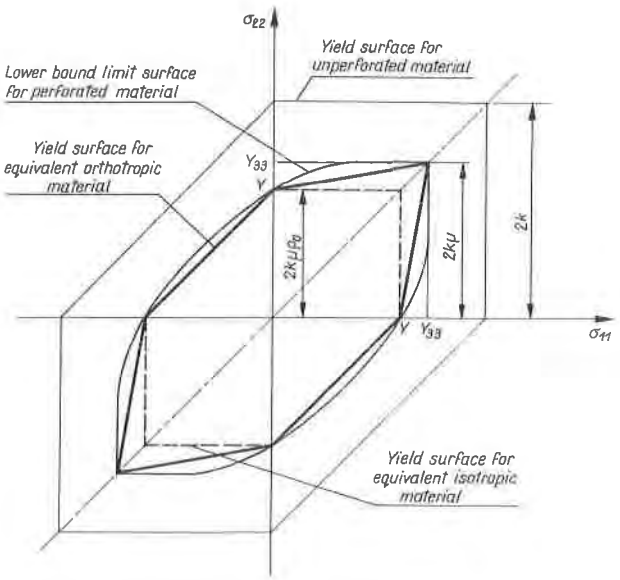

FIGURE 3 THE CONCEPT OF EQUIVALENT ORTHOTROPIC MATERIAL APPLIED TO PERFORATED SHEETS

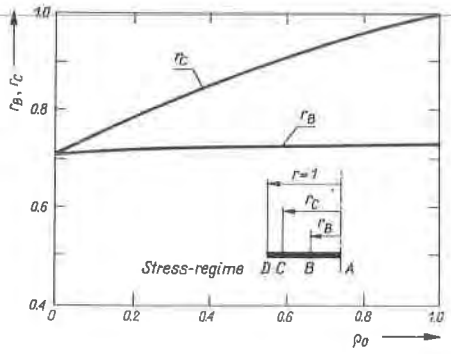

FIGURE 4 DIMENSIONLESS RADII OF INTERFACES BETWEEN THE STRESS REGIMES IN BUILT-IN PLATE

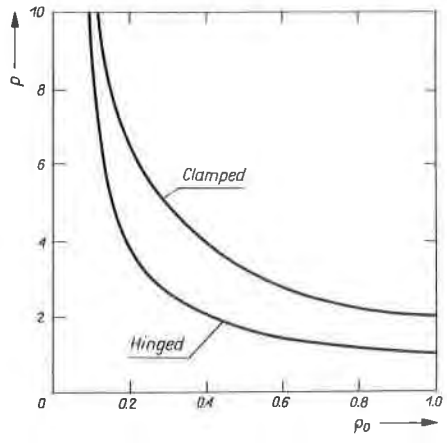

FIGURE 5 COLLAPSE PRESSURE FOR PERFORATED PLATE MADE OF AN EQUIVALENT ORTHOTROPIC MATERIAL

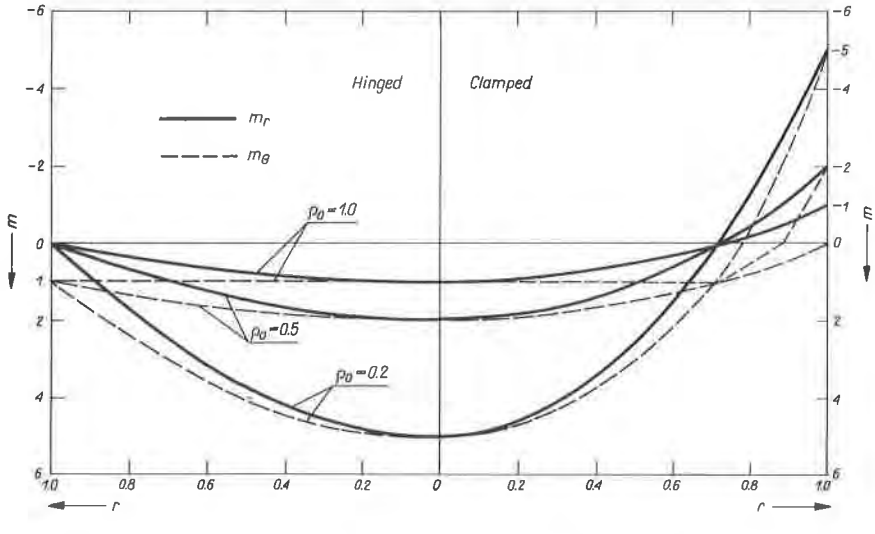

FIGURE 6 RADIAL AND CIRCUMFERENTIAL MOMENT DISTRIBUTIONS IN ORTHOTROPIC CIRCULAR PLATE AT COLLAPSE

/$Y_{11} = Y_{22} = Y$; $Y_{33} = \varrho_0 \cdot Y$/

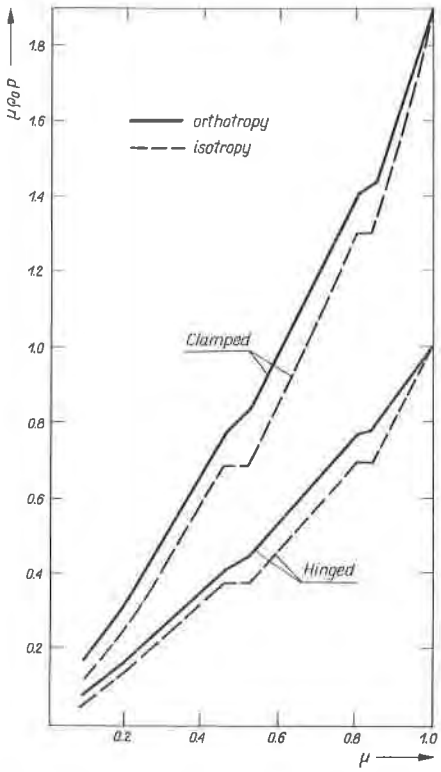

FIGURE 7 COLLAPSE PRESSURES FOR PLATES MADE OF EQUIVALENT ISOTROPIC AND ORTHOTROPIC MATERIALS
/TRIANGULAR PENETRATION PATTERN/